nature climate change

Article

https://doi.org/10.1038/s41558-026-02670-5

Global heat stress intensification and its expanding footprint on the human population

Received: 20 January 2026

Accepted: 19 May 2026

Published online: 22 June 2026

Check for updates

Rebecca Emerton [1] ✉, Julien Nicolas [2], Anna Lombardi [2] & Claudia Di Napoli [1]

Climate warming is driving more frequent and intense heat extremes. Yet, changes in heat stress, the leading cause of weather-related mortality, remain poorly quantified at the global scale. Here, using the Universal Thermal Climate Index, we assess heat stress globally since 1950, examining daytime extremes, nocturnal heat and compound daytime–nighttime events, revealing a pronounced, multidimensional intensification. Extreme 'feels-like' temperatures have become more frequent on every continent, and the spatial footprint of hazardous heat has expanded, exposing previously unaffected regions. Heat stress days and tropical nights have increased, with some regions experiencing up to 50 additional heat stress days annually and an extended heat stress season. The hottest nights of the year are warming faster (0.32 °C per decade) than the hottest days (0.27 °C), and compound events are more frequent, severe and prolonged. Population exposure to dangerous heat has increased markedly, driven by intensifying heat stress in addition to population growth.

Heat is the leading cause of weather-related mortality worldwide and exacerbates underlying illnesses such as cardiovascular, respiratory and mental health conditions[1]. As global warming intensifies, heatwaves are becoming more frequent, longer and more severe[2–4], further increasing the risk of heat-related illness and death[5]. One quarter of heatwaves between 2000 and 2019 were virtually impossible without climate change[6]. Yet, while trends in heatwaves are well documented, many people worldwide are exposed to chronic heat[7], and less is known about how these changes translate into trends of heat as experienced by the human population, particularly at the global scale.

Thermal stress indices quantify heat stress, defined as the net heat load on an individual, accounting for environmental and personal parameters[8]. Due to the nonlinearity of these indices, whereby equal warming at higher temperatures leads to a greater increase in thermal indices, perceived temperatures are rising faster than air temperature[9]. Here, we use the Universal Thermal Climate Index (UTCI), a widely adopted biometeorological thermal stress index[10] accounting for temperature, humidity, wind and radiation, alongside modelling how the human body responds to the environment. Expressed as a 'feels-like' temperature (°C), the UTCI classifies ten categories of cold to extreme heat stress, based on impacts on the human body[11].

The ERA5-HEAT reanalysis[12,13] provides globally consistent UTCI data from 1940 to the present, enabling long-term, transboundary assessment of trends. Recent analysis[14] revealed mean UTCI increases of up to 2.5 °C across North America, Europe and Asia in 1991–2020 compared with 1941–1970[14,15]. These patterns highlight the need for a comprehensive global assessment of evolving heat stress extremes, including their intensity, frequency and duration, which is addressed in this work.

Using ERA5-HEAT, we examine changes in heat stress across the globe from 1950 to 2024 and contrast recent conditions (2015–2024) with the 1970s, the point from which heat stress indicators have risen markedly at the global scale. We assess trends in maximum and minimum feels-like temperatures on the hottest days of each year and quantify the occurrence of strong (UTCI ≥32 °C), very strong (UTCI ≥38 °C)

[1]European Centre for Medium-Range Weather Forecasts, Reading, UK. [2]European Centre for Medium-Range Weather Forecasts, Bonn, Germany.
✉e-mail: rebecca.emerton@ecmwf.int

https://doi.org/10.1038/s41558-026-02670-5

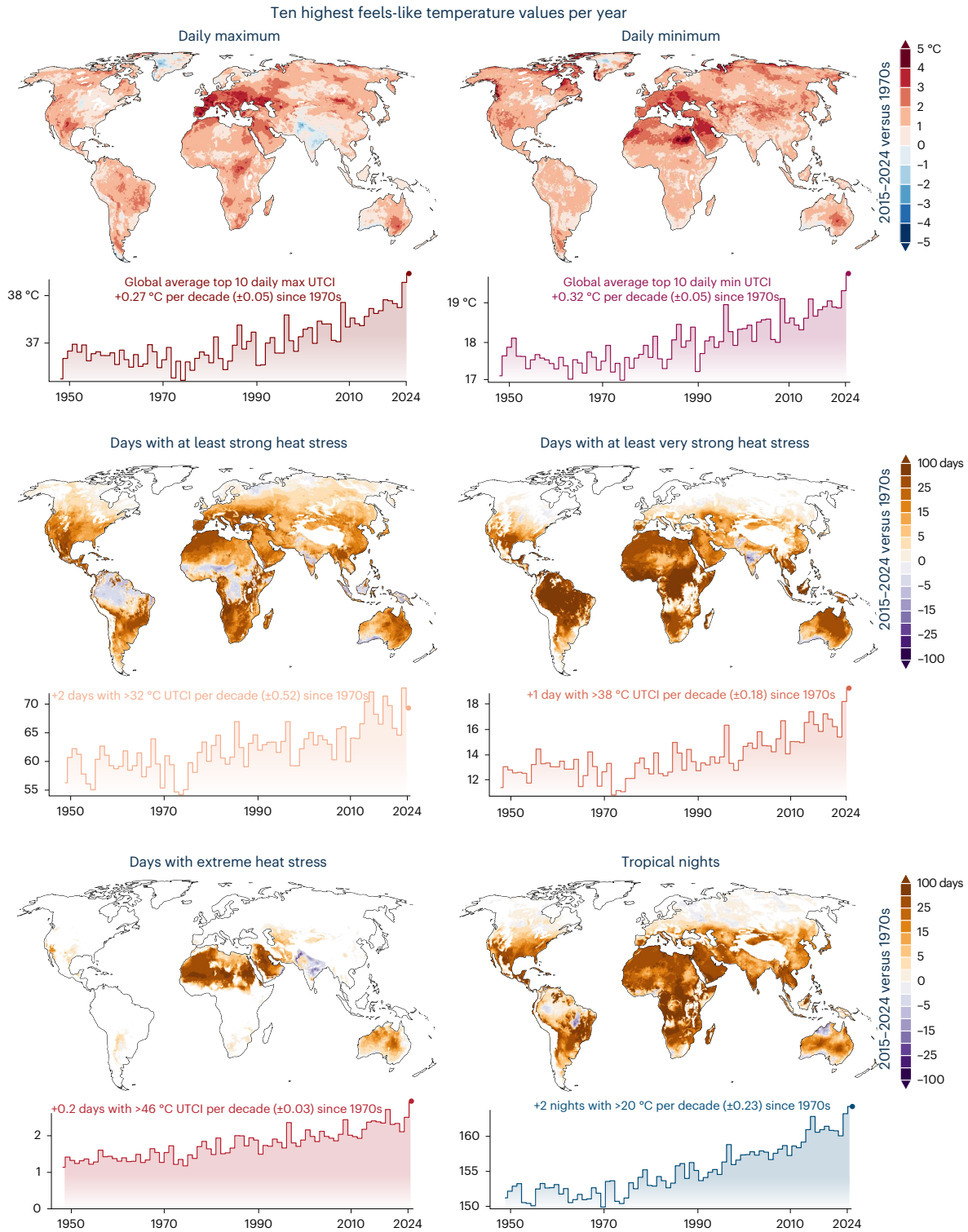

Fig. 1 | Changes in feels-like temperatures, heat stress days and tropical nights over time. Maps show the difference between the 1970s and the last 10 years (2015–2024) for indicators of heat stress, based on decadal averages of: the 10 highest daily maximum feels-like temperature values per year (UTCI, °C), the 10 highest daily minimum feels-like temperature values per year (UTCI, °C), the annual number of days with at least strong (UTCI ≥32 °C), very strong (UTCI ≥38 °C) and extreme (UTCI ≥46 °C) heat stress, and annual number of tropical nights (minimum temperature ≥20 °C). Line charts show the global average for each indicator for each year from 1950 to 2024. Trends per decade since the 1970s (1970–2024) are indicated above each chart, with 95% confidence intervals. All trends are statistically significant ($P < 0.001$). Trends were estimated using ordinary least-squares regression with HAC errors; P values are based on two-sided tests of the slope. No adjustment for multiple comparisons was applied. Basemap data from Natural Earth (https://www.naturalearthdata.com).

and extreme (UTCI ≥46 °C) heat stress. Because high nighttime temperatures amplify health risks by limiting recovery and increasing mortality[16], we also analyse the evolution of tropical nights (minimum temperature ≥20 °C). We characterize tropical nights by severity of nocturnal heat stress, and investigate compound events[9,17] that couple daytime and nighttime heat.

To link physical trends to societal impacts, we combine UTCI data with global demographic data[18] to quantify population exposure to

https://doi.org/10.1038/s41558-026-02670-5

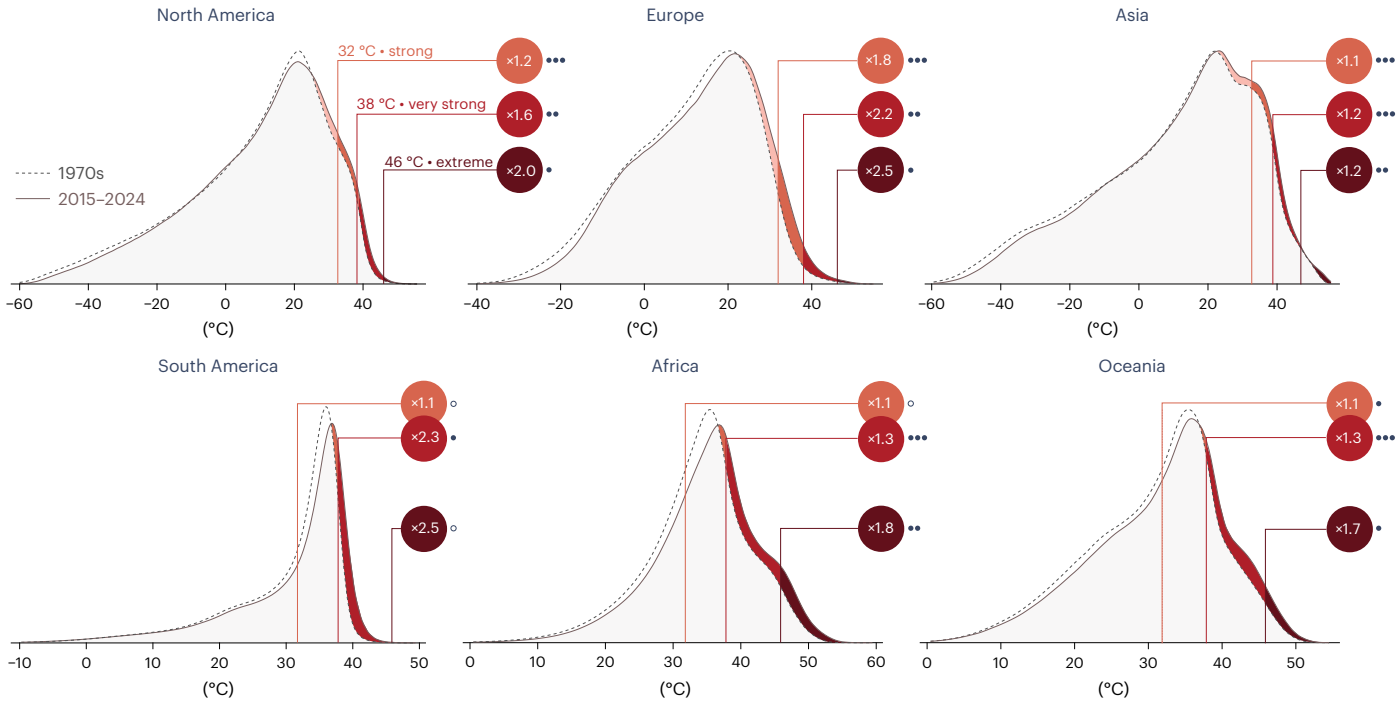

Fig. 2 | Frequency distribution of feels-like temperatures (UTCI) for each continent and increase from the 1970s to the last 10 years. Frequency is defined as the total number of occurrences, calculated as the sum across all grid cells and days within 2 periods: the 1970s and the last 10 years (2015–2024). Thresholds for strong (32 °C), very strong (38 °C) and extreme (46 °C) heat stress are highlighted, together with multiplication factors showing how much more often these thresholds were exceeded in 2015–2024 than in the 1970s. Statistical significance is indicated by the dots: $P < 0.001$ (•••), $P < 0.01$ (••), $P < 0.05$ (•). An open circle indicates $P > 0.05$. Statistical significance was assessed using a two-sided paired *t*-test comparing per-bin frequency counts above each threshold between the 1970s and the last 10 years (paired across temperature bins). Multiplication factors are computed from the summed counts above each threshold. No adjustment for multiple comparisons was applied. All but 3 values are statistically significant ($P < 0.05$), and 6 are highly statistically significant ($P < 0.001$). As the distributions represent aggregated counts over large, gridded regions, absolute values are complex and not directly interpretable; the focus is on the shape and shift of the distributions over time, and the *y* axis is therefore omitted. A version with the *y* axis included is provided in Extended Data Fig. 2. The shaded areas highlight the shift of the distributions towards more extreme values.

heat stress and how the number of people experiencing hazardous thermal conditions has evolved. We further attribute changes in exposure to the relative influences of population growth versus changes in heat stress.

Our analysis reveals a multidimensional intensification of heat stress worldwide, with implications for human exposure.

Heat stress trends at the global scale

Global average indicators of feels-like temperatures, heat stress days and tropical nights have all risen markedly since the 1970s (Fig. 1). The maximum feels-like temperature on the ten warmest days of the year has increased by 0.27 ± 0.05 °C per decade since the 1970s, while the ten warmest nighttime minima have risen even faster, at 0.32 ± 0.05 °C per decade. These trends translate to an additional two days per decade with at least strong heat stress, one with at least very strong heat stress and two additional tropical nights.

Building on these trends, we map changes across the globe, comparing the most recent decade (2015–2024) with the 1970s to capture the magnitude of change (Fig. 1).

Daily maximum feels-like temperatures on the ten warmest days of the year have increased across most regions, with the strongest warming in Europe, northern Africa and the Arabian Peninsula—up to 4 °C, and locally 5 °C—warmer in the last 10 years than in the 1970s. Elsewhere, increases of 2–3 °C dominate, although small areas in Greenland, coastal southwestern Australia and parts of India and Pakistan show decreases of 1–3 °C. Research supports the decreasing trend in the UTCI in parts of India[19–22]. The warmest nighttime minima have risen almost everywhere, including regions with slight daytime cooling. The largest increases occur in the northern extratropics: up to 6 °C in northwestern North America and northern Canada, 5 °C in northern Africa, and 4 °C in Europe and the Arabian Peninsula.

Heat stress days and tropical nights have proliferated globally. The spatial footprint of heat stress has also expanded, meaning that regions previously untouched by extreme heat are now affected (Extended Data Fig. 1). Subtropical regions, including in southern North America, southern Europe, northern and southern Africa, and South America, now experience up to 50 more days per year with at least strong heat stress. Many of these areas also see more days with very strong heat stress, and some places, such as in northern Africa, the Arabian Peninsula, Australia and parts of western North America have also seen an increase in extreme heat stress days. In the tropics, strong heat stress typically remains nearly year-round, but there are shifts towards the more severe categories. Exceptions include parts of India, Pakistan and coastal southwestern Australia, where heat stress days have declined, although India and Pakistan are experiencing more tropical nights.

Changes in the frequency and duration of heat stress

On every continent, feels-like temperatures are more frequently exceeding thresholds for very strong and extreme heat stress in our current climate (2015–2024) compared with the 1970s (Fig. 2). Extreme heat stress, at which point urgent action is required to prevent severe health impacts[11], now occurs 2.5 times more often in Europe and South America, twice as often in North America and 1.8, 1.7 and 1.2 times more often in Africa, Oceania and Asia, respectively. Extended Data Table 1

https://doi.org/10.1038/s41558-026-02670-5

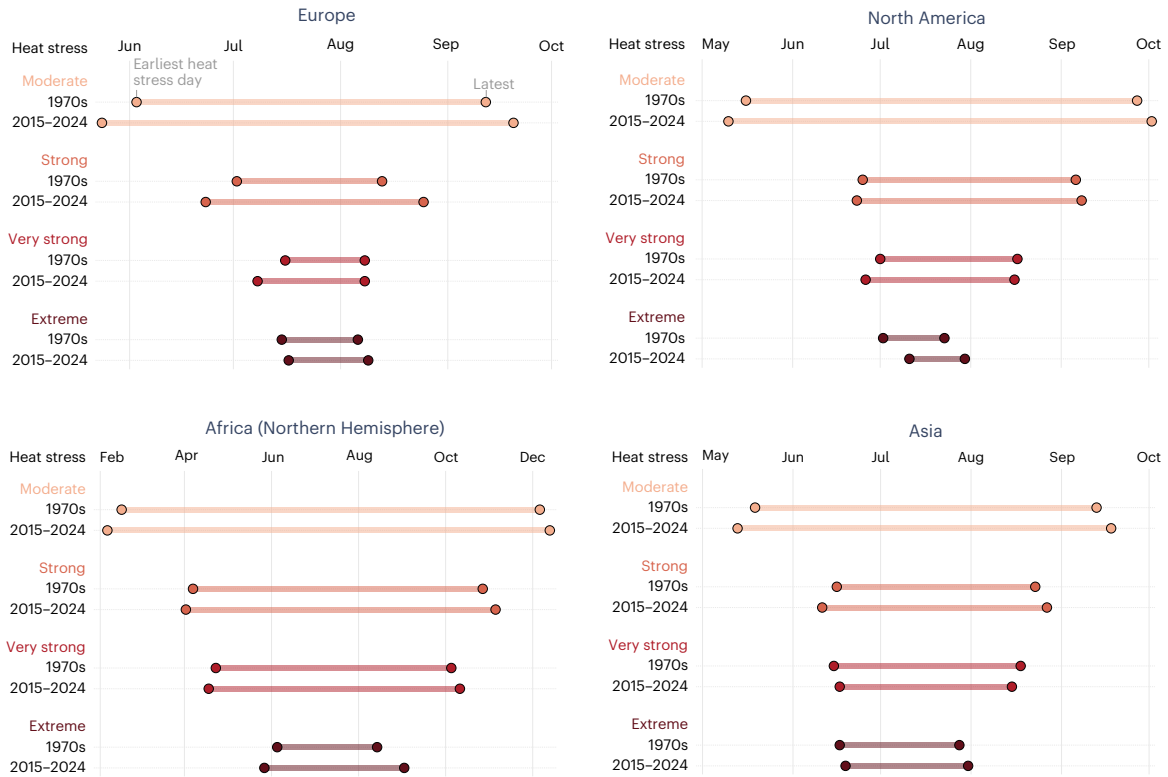

Fig. 3 | Change in the duration of the heat stress season. For each continent in the Northern Hemisphere, the average earliest and latest heat stress day of the year, for four heat stress thresholds (moderate (≥26 °C UTCI), strong (≥32 °C UTCI), very strong (≥38 °C UTCI) and extreme (≥46 °C UTCI) heat stress), in the 1970s and in the last 10 years (2015–2024). Due to the year-round presence of lower categories of heat stress in the tropics and less defined seasonality, the tropics are excluded from this analysis.

provides the equivalent frequency changes for the Intergovernmental Panel on Climate Change Sixth Assessment Report reference regions.

Although extreme heat stress remains rare in Europe, affecting 0.2% of days and locations in the last 10 years, this represents a 138% relative increase from 0.08% in the 1970s. In Africa, the frequency has risen from 4.1% to 7.4%, the highest of any continent. Africa also records the greatest overall heat stress burden, with a strong heat stress frequency of 70% in the past decade, compared with 63% in South America, 55% in Oceania, 24% in Asia, 15% in North America and 9% in Europe.

Across all continents, the largest relative increases in frequency occur in the most severe heat stress categories.

In the Northern Hemisphere, the season during which heat stress is experienced has increased in duration (Fig. 3). Averaged across the northern extratropics, the first and last days with moderate heat stress now span a season 15 days longer than in the 1970s. For strong heat stress, the season is an average of 12 days longer; for very strong, 9 days; and for extreme, 6 days.

Europe and Africa (Northern Hemisphere) show the longest season extensions. In Europe, moderate heat stress now begins on average in mid-May rather than early June and persists until nearly October, while strong heat stress starts in June instead of July. For these levels of heat stress, the shortest heat stress season in the last 10 years was longer than the longest season in the 1970s (Extended Data Fig. 3). Similar, although less pronounced, trends occur in Africa, North America and Asia. In Africa, the extreme heat stress season has lengthened by 28 days—the largest increase observed, with the shortest extreme heat stress season in the last 10 years lasting 11 days longer than the longest season in the 1970s Elsewhere, the extreme heat stress season remains similar in duration but shifts later, most notably in North America, where it begins 10 days later and ends 7 days later than in the 1970s.

Compound heat stress days and tropical nights

Rising nighttime feels-like temperatures underscore the need to assess not only the occurrence of tropical nights but also the intensity of heat stress they impose. Here, we classify tropical nights by the heat stress category of their minimum overnight UTCI (Fig. 4).

There is a decreasing trend in the number of tropical nights with no heat stress (UTCI <26 °C) since the 1970s, accompanied by an increasing trend in the number of tropical nights with moderate or strong heat stress. The proportion of tropical nights with moderate heat stress peaked at 11.4% in 2024, the warmest year on record for the globe, up from a minimum of 2.2% in 1965. Before 1998, a strong El Niño year[23,24], the share never exceeded 5.8%.

Strong heat stress on tropical nights was virtually absent before 1998 (≤0.02%) and remained at or below 0.04% until 2023, but rose to 0.08% in 2024. No tropical nights have yet recorded very strong or extreme heat stress.

More frequent heat stress days and tropical nights are driving an increase in compound heat events (Fig. 5), which globally have become more frequent and prolonged, especially in Europe, Africa and North America.

In Europe, the occurrence of single-day compound events (one heat stress day followed by one tropical night) has increased by 73% since the 1970s. Events lasting 15–30 days are now 3.4 times more common, and the longest observed durations—up to 120 consecutive days—have almost doubled in frequency.

In Africa (Northern Hemisphere), shorter-duration compound events (1–90 days) have declined as sequences of up to a full year (271–365 days) have increased by a factor of 2.8. In the Southern Hemisphere, Africa has seen increases across all durations, with the longest events (181–270 days) now occurring 2.8 times more frequently. Asia and Oceania exhibit smaller changes, with

https://doi.org/10.1038/s41558-026-02670-5

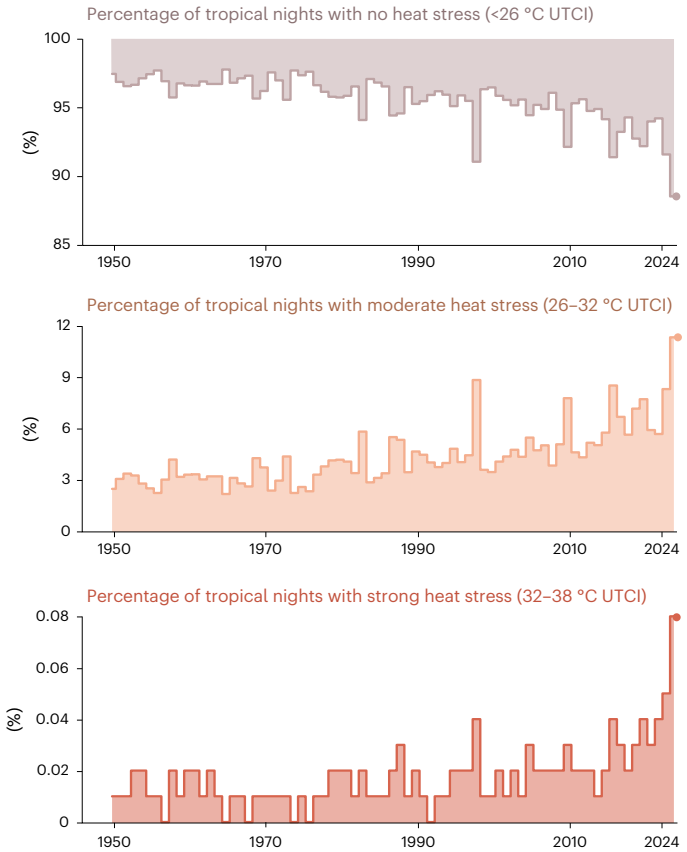

Fig. 4 | Severity of heat stress on tropical nights, from 1950 to 2024. Globally, the annual percentage of tropical nights with no heat stress (<26 °C UTCI), moderate heat stress (26–32 °C UTCI) and strong heat stress (32–38 °C UTCI), based on the daily minimum UTCI during the tropical night.

modest increases for most durations and larger increases for the longest events.

Population exposure to heat stress

Population exposure to heat stress has increased in recent decades, driven by rising frequency, intensity and duration of heat stress alongside population growth and redistribution (Fig. 6). Comparing exposure by heat stress severity and duration in the last 10 years (2015–2024) with the 1970s reveals that increases are steepest for the most severe categories and longest durations, meaning more people are exposed, for more days, and to more intense heat stress.

In the 1970s, 55% of the global population experienced at least 90 days of strong heat stress annually; this has risen to 70% in our current climate. Exposure to at least one day of extreme heat stress has grown from 16% to 22%; accounting also for the increase in population, this represents an additional one billion people. For most categories, the increase in exposure caused by changes in heat stress is equal to or larger than the increase caused by population growth and redistribution. This may be further amplified by the spatial variability of population growth, with some of the largest increases occurring in regions with hot climates[25].

Mapping annual person-days of exposure to very strong heat stress in the last 10 years (Extended Data Fig. 4) identifies regions of greatest population exposure, including sub-Saharan Africa, South and Southeast Asia, the Arabian Peninsula and the Mediterranean.

Given ERA5-HEAT limitations in capturing extremes and microclimates such as urban heat islands[26], these estimates are likely to be conservative, particularly for cities. They also draw on a hybrid gridded population dataset that, while providing long-term coverage, carries uncertainties in early-period and regional population distributions.

Discussion and conclusions

This study provides insights into changes in the frequency, severity and duration of heat stress with climate change, and a comprehensive global-scale analysis of not only daytime extremes but also nocturnal heat and compound daytime–nighttime events. Our analysis is based on the UTCI; by incorporating the combined effects of temperature, humidity, wind and radiation, and how the human body responds to the thermal environment, the UTCI offers a physiologically relevant measure of thermal stress. We demonstrate a clear and accelerating climate-driven intensification of heat stress since the 1970s, with implications for the health of billions of people worldwide.

Feels-like temperatures have risen markedly, with nighttime minima increasing faster (global average of 0.32 ± 0.05 °C per decade since the 1970s) than daytime maxima (0.27 ± 0.05 °C per decade). These changes translate into more frequent and severe heat stress days and, in the Northern Hemisphere, a prolonged heat stress season. Importantly, the most dramatic shifts often occur at the highest thresholds of heat stress, where health risks are greatest. The spatial footprint of hazardous heat stress has expanded, exposing previously unaffected regions and posing adaptation challenges not only in areas where heat stress is becoming more extreme, but also in those where it has historically not been experienced.

Population exposure has increased across all categories and durations of heat stress, compounded by population growth. In the 1970s, 55% of the global population experienced at least 90 days of strong heat stress annually; this has risen to 70% in our current climate. Exposure to at least one day of extreme heat stress has increased from 16% to 22%, representing an additional one billion people who now experience extreme heat stress annually compared with the 1970s. In the future, exposure to heat stress will continue to increase, with the largest absolute increases in low-latitude regions, and the largest relative increases in high-latitude regions[27]. A recent United Nations Children's Fund report[28] highlights that around 559 million children are already exposed to high heatwave frequency, and that virtually every child on Earth is forecast to face more frequent heatwaves by 2050, even if global warming is kept below 2 °C above the pre-industrial level, as agreed in the 2015 Paris Agreement. Extreme heat can be particularly life-threatening to young children, as they are less able to regulate their body temperature[28].

Our findings also reveal previously unquantified aspects of heat stress at the global scale, focussing on changes in compound heat stress days and tropical nights. Periods of heat stress during the day with little relief overnight can have severe implications for health and mortality, and the evidence indicates that the duration of exposure to heat stress is an important factor for human health[29]. We demonstrate that the number of tropical nights with no heat stress is declining, due to an increasing proportion of nights in which feels-like temperatures still exceed heat stress thresholds.

We show that compound events combining consecutive heat stress days and tropical nights have become more frequent and prolonged on every continent, with the most dramatic changes in Europe and Africa. These patterns underscore the growing importance of heat stress dynamics beyond just daytime extremes.

The observed rise in compound events aligns with emerging evidence that concurrent daytime and nighttime heat poses disproportionate health risks due to the absence of nocturnal cooling[30,31]. Our classification of tropical nights by heat stress severity adds further insight to this understanding, revealing that nocturnal heat is not only more frequent but also more intense.

Our findings complement previous work on heatwave trends under anthropogenic warming[5,6,32–34] and extend our understanding by using the UTCI and considering heat stress year-round rather than confined to specific events, given the exposure of many people worldwide, predominantly in the tropics, to chronic heat[7]. While most global assessments focus on air temperature, our use of the UTCI reveals

https://doi.org/10.1038/s41558-026-02670-5

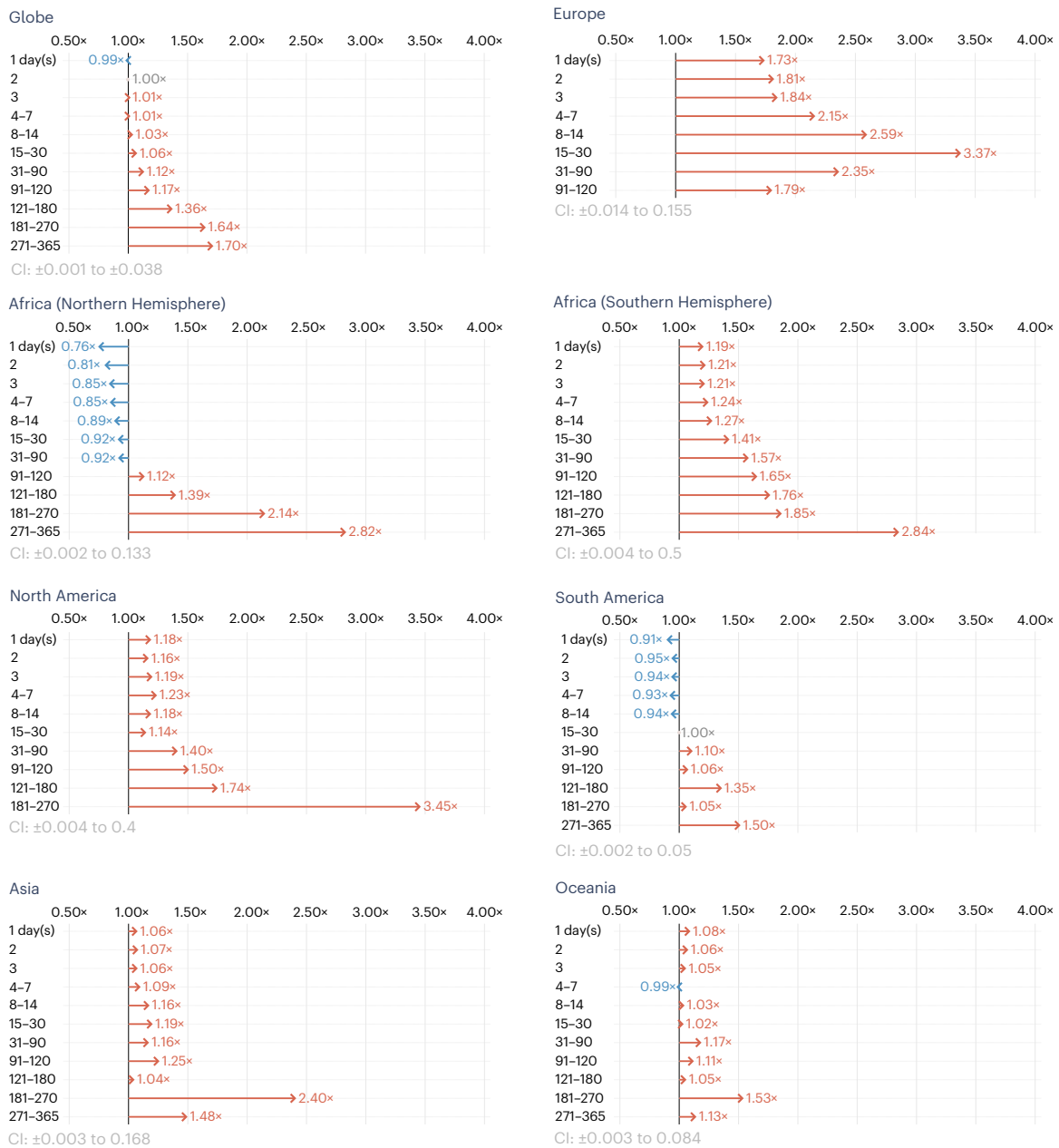

Fig. 5 | Change in frequency of consecutive compound heat stress days and tropical nights between the 1970s and the last 10 years (2015–2024). Based on the multiplication factor, indicating how many times greater the frequency was in the last 10 years compared with the 1970s. Changes are indicated for a range of periods of consecutive heat stress days and tropical nights, from 1 (1 day and 1 night) to 271–365. Longer periods are omitted when no compound events of that length are recorded. Values >1 (red) indicate an increased frequency in the last 10 years compared with the 1970s, and values <1 (blue) indicate a decreased frequency. Uncertainty increases for longer compound event durations due to smaller sample sizes. The 95% CI around the multiplication factors therefore widen with increasing duration. The confidence intervals for the shortest and longest duration for each continent are noted, and a table of confidence intervals for each event duration is provided in Extended Data Table 2. Heat stress days are defined as those with at least strong heat stress (≥32 °C UTCI).

additional dimensions driven not only by changes in temperature but also by changes in humidity, wind and radiation. This distinction is critical: recent studies[9,30] show that the nonlinearity of thermal indices means they change at a different rate than air temperature alone and, in some cases, may diverge from temperature trends—for example, in parts of India, where daytime feels-like temperatures have decreased since the 1970s while nighttime minima have increased.

Increasing heat stress and exposure has profound implications for climate adaptation and public health. Heat stress is already the leading cause of weather-related mortality[1,35,36], and our results show that the dangers continue to increase. Adaptation strategies must address both daytime and nighttime heat. Heat-health action plans, early warnings systems and urban cooling interventions are essential to reduce exposure. Integrating heat stress metrics into climate risk assessments and adaptation strategies is vital, as temperature-based thresholds may underestimate risk in humid or low-wind environments. At present, adaptive capacity varies across regions and populations, but such adaptation strategies may help to reduce vulnerability.

While this study focuses on historical trends to understand how our current climate differs from that of recent decades, projections under different emissions scenarios are urgently needed to inform

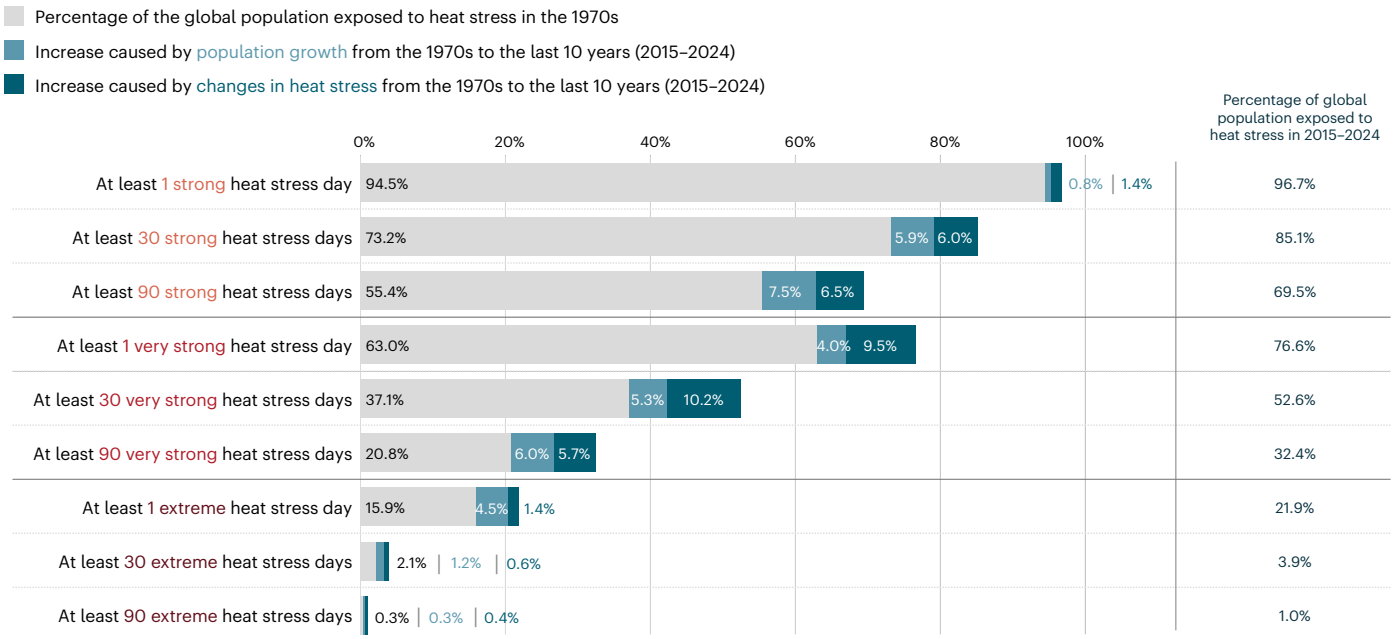

Fig. 6 | Increase in the percentage of the global population exposed to heat stress from the 1970s to the last 10 years (2015–2024). For strong (UTCI ≥32 °C), very strong (UTCI ≥38 °C) and extreme (UTCI ≥46 °C) heat stress thresholds, and durations of at least 1, 30 and 90 days of each level of heat stress, the percentage of the population exposed to each threshold and duration of heat stress in the 1970s is indicated (grey bars), alongside the increase caused by population growth from the 1970s to the last 10 years (light-blue bars) and the increase caused by heat stress changes (teal bars). The total percentage of the population exposed to each threshold and duration of heat stress in the last 10 years is indicated on the right. Based on a total global population of 4.06 billion people in 1975 and 7.77 billion in 2020.

long-term adaptation planning. At present, consistent global climate projections for the UTCI do not exist; future work should endeavour to produce and assess such projections. Recent research into exposure to wet-bulb temperature found that humanity is more vulnerable to moist heat stress than had previously been proposed, and that in the future, moist heat extremes will lie outside the bounds of human experience and beyond current mitigation strategies for billions of people[29]. High-resolution datasets will also be critical for quantifying urban heat stress for example. While current state-of-the-art reanalyses such as ERA5-HEAT have been found to be suitable and useful for climate and health studies[26], they cannot fully resolve microclimates such as urban heat islands. Our estimates may therefore underrepresent extremes and population exposure, particularly for cities. In addition, the UTCI models thermal stress for a standardized reference individual and does not account for individual variability, including differences in age, body composition or acclimatization.

Overall, our findings reveal a multidimensional intensification of heat stress, and an increase in exposure that exceeds the effect of population growth alone. Exposure is increasing across all severity thresholds, as the magnitude, frequency and duration of heat stress all increase, both during the day and at night. These changes pose escalating threats to health, livelihoods and economic productivity worldwide. Without urgent mitigation and adaptation, billions more people may face dangerous heat stress conditions in the coming decades. These comprehensive results represent important considerations for climate policy and planning that are essential to safeguard human health in a warming world.

Online content

Any methods, additional references, Nature Portfolio reporting summaries, source data, extended data, supplementary information, acknowledgements, peer review information; details of author contributions and competing interests; and statements of data and code availability are available at https://doi.org/10.1038/s41558-026-02670-5.

References

1. *Heat and Health* (World Health Organization, 2024); https://www.who.int/news-room/fact-sheets/detail/climate-change-heat-and-health
2. Domeisen, D. I. V. et al. Prediction and projection of heatwaves. *Nat. Rev. Earth Environ*. https://doi.org/10.1038/s43017-022-00371-z (2023).
3. Martinez-Villalobos, C. et al. Accelerating increase in the duration of heatwaves under global warming. *Nat. Geosci*. https://doi.org/10.1038/s41561-025-01737-w (2025).
4. Perkins, S. E., Alexander, L. V. & Nairn, J. R. Increasing frequency, intensity and duration of observed global heatwaves and warm spells. *Geophys. Res. Lett*. https://doi.org/10.1029/2012GL053361 (2012).
5. Callahan, C. W. et al. Increasing risk of mass human heat mortality if historical weather patterns recur. *Nat. Clim. Change* **16**, 26–32 (2026).
6. Quilcaille, Y. et al. Systematic attribution of heatwaves to the emissions of carbon majors. *Nature* **645**, 392–398 (2025).
7. Cruz, M. et al. Where heat does not come in waves: a framework for understanding and managing chronic heat. *Environ. Res. Clim.* **4**, 023002 (2025).
8. McGregor, G. R. & Vanos, J. K. Heat: a primer for public health researchers. *Public Health* **161**, 138–146 (2018).
9. Zhu, J., Wang, S. & Fischer, E. M. Increased occurrence of day–night hot extremes in a warming climate. *Clim. Dyn.* **59**, 1297–1307 (2022).
10. Jendritzky, G., de Dear, R. & Havenith, G. UTCI—why another thermal index? *Int. J. Biometeorol.* **56**, 421–428 (2012).
11. Di Napoli, C., Pappenberger, F. & Cloke, H. L. Verification of heat stress thresholds for a health-based heatwave definition. *J. Appl. Meteorol. Climatol.* **58**, 1177–1194 (2019).
12. Di Napoli, C. et al. Thermal comfort indices derived from ERA5 reanalysis. *Copernicus Climate Change Service (C3S) Climate Data Store* https://doi.org/10.24381/cds.553b7518 (2020).

13. Di Napoli, C. et al. ERA5-HEAT: a global gridded historical dataset of human thermal comfort indices from climate reanalysis. *Geosci. Data J.* **8**, 2–10 (2020).
14. Hamed, M. M., Alasow, A. A. & Shahid, S. Global trends in human thermal stress: a spatiotemporal analysis from 1940 to 2020. *Earth Syst. Environ.* **9**, 2529–2541 (2024).
15. Mărmureanu, L. et al. Changes in the thermal stress across Europe between 1940–2023. *Int. J. Biometeorol.* **69**, 3569–3586 (2025).
16. Roye, D. et al. Short-term association between hot nights and mortality: a multicountry analysis in 178 locations considering hourly ambient temperature. *Environ. Int.* **203**, 109719 (2025).
17. Chen, Y. & Zhai, P. Revisiting summertime hot extremes in China during 1961–2015: overlooked compound extremes and significant changes. *Geophys. Res. Lett.* **44**, 10 (2017).
18. Chambers, J. Hybrid gridded demographic data for the world, 1950–2020. *Zenodo* https://doi.org/10.5281/zenodo.3768003 (2020).
19. Naskar, P. R. et al. Spatiotemporal variations of UTCI based discomfort over India. *J. Earth Syst. Sci.* **133**, 47 (2024).
20. Park, J. et al. Aerosol-induced surface cooling elevates relative humidity in the Indo-Gangetic Plain. *Commun. Earth Environ.* https://doi.org/10.1038/s43247-025-02513-9 (2025).
21. Liu, J. et al. CO_2 radiative forcing induces summer cooling over India. *Nat. Commun.* **17**, 2724 (2026).
22. Sarin, T. S. & Vinoj, V. Assessing the relationship between atmospheric aerosols and maximum surface air temperature over the Indian region. *Sci. Rep.* https://doi.org/10.1038/s41598-026-40641-0 (2026).
23. Copernicus Climate Change Service. Global climate highlights 2024. *ECMWF* https://climate.copernicus.eu/global-climate-highlights-2024 (2025).
24. McPhaden, M. J. Genesis and evolution of the 1997–98 El Niño. *Science* **283**, 950–954 (1999).
25. Gu, D., Andreev, K. & Dupre, M. E. Major trends in population growth around the world. *China CDC Wkly* https://doi.org/10.46234/ccdcw2021.160 (2021).
26. Urban, A. et al. Evaluation of the ERA5 reanalysis-based Universal Thermal Climate Index on mortality data in Europe. *Environ. Res.* **198**, 111227 (2021).
27. Xu, X. et al. Increasing meridional disparity of population exposure to heat stress. *Geogr. Sustain.* **7**, 100391 (2025).
28. United Nations Children's Fund. *The State of the World's Children 2024: The Future of Childhood in a Changing World* (UN, 2024); https://doi.org/10.18356/9789211069631
29. Vecellio, D. J. et al. Greatly enhanced risk to humans as a consequence of empirically determined lower moist heat stress tolerance. *Proc. Natl Acad. Sci. USA* **120**, e2305427120 (2023).
30. Liu, J. et al. Nonlinear exposure–response associations of daytime, nighttime, and day–night compound heatwaves with mortality amid climate change. *Nat. Commun.* **16**, 624 (2025).
31. Yang, J. et al. Drivers of associations between daytime–nighttime compound temperature extremes and mortality in China. *Nat. Commun. Med.* **4**, 125 (2024).
32. Perkins-Kirkpatrick, S. E. & Gibson, P. B. Changes in regional heatwave characteristics as a function of increasing global temperature. *Sci. Rep.* **7**, 12256 (2017).
33. Rogers, C. D. W. et al. Sixfold increase in historical northern hemisphere concurrent large heatwaves driven by warming and changing atmospheric circulation. *J. Clim.* **35**, 1063–1078 (2022).
34. Seneviratne, S. I. et al. in *Climate Change 2021—The Physical Science Basis* (eds Masson-Delmotte, V. P. et al.) 1513–1766 (IPCC, Cambridge Univ. Press, 2021); https://doi.org/10.1017/9781009157896.013
35. Romanello, M. et al. The 2023 report of the Lancet Countdown on health and climate change: the imperative for a health-centred response in a world facing irreversible harms. *Lancet* **402**, 2346–2394 (2023).
36. *European State of the Climate 2023* (Copernicus Climate Change Service & World Meteorological Organization, 2024); https://doi.org/10.24381/bs9v-8c66

Methods

Data

Reanalyses of temperature and thermal stress. Reanalysis datasets combine observational data with state-of-the-art models to 'fill in the gaps' where observations are scarce or absent, providing globally consistent datasets of past weather and climate. The ERA5[37–39] and ERA5-HEAT[12,13] reanalyses are used here to allow long-term and transboundary assessment of thermal stress trends. They provide global (excluding Antarctica, for ERA5-HEAT) hourly data from 1940 to near-real time at a 0.25° grid resolution. The variables used are 2-m air temperature from ERA5, and the UTCI from ERA5-HEAT. ERA5-HEAT combines air temperature, wind speed, radiation and dewpoint temperature (which, together with the air temperature, represents the humidity) from ERA5, and for any combination of these, the UTCI is defined as the air temperature of a reference outdoor environment that would elicit in the human body the same physiological model's response (sweat production, shivering, skin wettedness, skin blood flow and rectal, mean skin and face temperatures) as the actual environment[12]. It therefore represents a feels-like temperature in degrees Celsius.

The UTCI categorizes thermal stress on the basis of the feels-like temperature and corresponding physiological responses. Throughout this study, we use these established thresholds for at least moderate (26 °C), strong (32 °C), very strong (38 °C) and extreme (46 °C) heat stress. These physiologically based thresholds are designed to be globally applicable, enabling a consistent and interpretable assessment of heat stress and trends globally, with direct relevance for heat-health applications and planning. The UTCI models thermal stress for a standardized reference individual, however, and does not account for individual variability, including differences in age, body composition or acclimatization.

Population data. The dataset used for the population exposure analysis presented here is the 'Hybrid gridded demographic data for the world, 1950–2020' dataset[18], which provides 5-year population bands at a 0.25° grid resolution. This dataset is chosen due to its consistent temporal and spatial coverage with the ERA5 dataset; the 0.25° resolution release of this dataset was designed explicitly for the purpose of matching ERA5. It combines the National Aeronautics and Space Administration (NASA) Socioeconomic Data and Applications Center (SEDAC) Gridded Population of the World version 4 dataset for 2000–2020 with the ISIMIP Histsoc gridded population data for 1950–1999 and the United Nations World Population Program demographic modelling data.

Methodology

Heat stress trends at the global scale. To conduct a comprehensive analysis of global heat stress trends, a range of heat stress indicators were defined: (1) the average daily maximum UTCI on the 10 days with the highest daily maximum UTCI per year, (2) the average daily minimum UTCI on the 10 days with the highest daily minimum UTCI per year, (3) counts of heat stress days for different categories of heat stress, and (4) counts of tropical nights.

For (1) and (2), the daily maximum and minimum UTCI were extracted from the ERA5-HEAT dataset for each grid cell. For each year from 1950 to 2024, the ten highest daily maximum values and the ten highest daily minimum values were identified, and their means were calculated to produce annual metrics representing the hottest days and nights. This approach enables a more robust characterization of changes in extreme UTCI conditions by increasing the sample size and reducing sensitivity to single-day anomalies, compared with using only the single hottest day or night of each year.

For (3), the daily maximum UTCI for each day of the year was compared with the thresholds for at least strong (≥32 °C), very strong (≥38 °C) and extreme (≥46 °C) heat stress in order to count the number of days per year exceeding these thresholds at each grid cell. This process was repeated for each year from 1950 to 2024. The methodology for (4) is similar. The daily minimum air temperature was extracted from ERA5 for each day and compared with the 20 °C threshold used to define a tropical night. The number of days per year on which the daily minimum temperature did not fall below 20 °C was counted.

All indicators are based on the maximum or minimum of the data during each 24-h period from 00:00 to 23:59 UTC; adjustments are not made for local time zones.

To produce a global annual time series for each indicator, the mean over all land grid cells was computed. The global trends indicated in Fig. 1 were estimated using least-squares linear regression of the annual values from 1970 to 2024, applied to each indicator, and multiplied by ten to express changes per decade.

Epochal differences. Based on the indicators described above, global maps of the differences between the 1970s and the most recent decade were created. The 1970s were chosen as the reference period because this marks the onset of a clear and sustained global trend in all indicators. The comparison between these two decades is therefore continued throughout the study.

To quantify the change in key heat stress indicators between the 1970s and the most recent decade, the decadal mean for the 1970s (1970–1979) and for the last 10 years (2015–2024) was calculated for each grid cell, and the former subtracted from the latter to obtain the spatial pattern of change.

This epochal differences approach provides a direct and temporally transparent measure of change. By contrasting two multiyear periods, it avoids the assumptions of linearity and temporal homogeneity inherent in long-term trend fitting, while suppressing the influence of interannual variability associated with the El Niño Southern Oscillation and other short-lived perturbations. In addition, because the method produces spatial fields representing concrete, absolute changes between two well-defined periods, it offers an intuitive and accessible way to convey changes in heat stress indicators that is both useful for scientific analysis and for communicating findings to a broad audience.

Changes in the frequency of heat stress. To examine changes in the frequency of occurrence of heat stress conditions for each continent, frequency distributions of daily maximum feels-like temperatures were computed using the UTCI. For all land grid cells within each continental domain, daily maximum UTCI values were extracted for two periods: the 1970s and the most recent decade (2015–2024). For each period, the total number of occurrences within successive 1 °C UTCI bins were calculated by summing counts across all grid cells and all days within each decade. This yields frequency distributions characterizing the frequency of the full range of feels-like temperatures experienced on each continent for each of the two decades considered.

To quantify changes in extreme heat, we computed the frequency with which the UTCI exceeds established thresholds for at least strong (32 °C), very strong (38 °C) and extreme (46 °C) heat stress. For each threshold and continent, the multiplication factor is defined as the ratio of exceedance frequencies in the last 10 years relative to the 1970s.

The continental domains used in this study are as follows: Europe 35–70° N, 25° W–45° E; North America 15–70° N, 170–50° W; Africa 35° S–38° N, 20° W–55° E; South America 60° S–15° N, 90–30° W; Asia 5–80° N, 45–180° E; Oceania 50° S–10° N, 110–180° E.

Changes in the duration of heat stress. To expand on the analysis of the changing frequency of heat stress, we assessed how both the timing and duration of heat stress have changed by analysing the length of the 'heat stress season' for each continent in the 1970s and in the most recent decade. The heat stress season is defined as the interval between the first and last days in a year on which UTCI exceeds thresholds for heat stress. For each year and for four UTCI thresholds

representing at least moderate (≥26 °C), strong (≥32 °C), very strong (≥38 °C) and extreme (≥46 °C) heat stress, we identified the earliest and latest exceedance dates for each grid cell.

Because seasonal cycles differ between hemispheres, exceedances were evaluated from January to December in the Northern Hemisphere and from July to June in the Southern Hemisphere. The tropics (20° N–20° S) were excluded because heat stress occurs throughout much of the year in tropical regions, meaning that a distinct season cannot be reliably defined.

For each continent, extratropical land grid cells were averaged to obtain the decadal mean onset and end dates for the heat stress season in the 1970s and in the last 10 years (2015–2024). Season duration was then calculated as the difference between these mean onset and end dates, allowing comparison of how the period of the year affected by different levels of heat stress has evolved over time.

Compound heat stress days and tropical nights. *Intensity of heat stress on tropical nights*. A key objective of this study was to assess changes not only in daytime heat extremes, but also in nocturnal heat, given that high nighttime temperatures amplify health risks by limiting recovery and increasing mortality[16]. To investigate this, we first classify tropical nights according to the severity of heat stress experienced.

For each day in the period from 1950 to 2024, ERA5 daily minimum air temperature was extracted and used to generate a binary mask identifying whether each land each grid cell experienced a tropical night (minimum temperature ≥20 °C).

Daily minimum UTCI from ERA5-HEAT was then extracted for the same period. For each day, the tropical night mask was applied to the UTCI field, retaining only those grid points that experienced a tropical night. For each year, the number of grid-cell-days (that is, all land grid cells across all days) falling within each UTCI heat stress category (no heat stress <26 °C, moderate 26–32 °C, strong 32–38 °C, very strong 38–46 °C and extreme ≥46 °C) was counted. These counts were then normalized by the total number of grid-cell-days with tropical nights in that year, producing the percentage of tropical nights during which minimum UTCI still exceeded thresholds for heat stress.

This approach allows characterization of the severity of nighttime heat conditional on tropical night occurrence, rather than conflating changes in overall tropical night frequency with changes in nocturnal heat stress intensity, and provides a clear measure of how often nights that are already warm also impose physiologically meaningful heat stress.

While the UTCI provides a physiologically based assessment of heat stress, the categories were originally developed for daytime conditions under typical solar and metabolic loads. As a result, applying these categories to nocturnal minimum UTCI introduces some limitations. At night, the absence of solar radiation, reduced activity levels and altered thermoregulatory dynamics mean that human heat strain may not correspond directly to the same UTCI threshold ranges used during the day. Consequently, the categorization applied here should be interpreted as an indicative measure of relative nocturnal heat stress severity for assessing changes in the intensity of warm nights. Future work should endeavour to evaluate the most appropriate physiologically relevant thresholds for nocturnal heat stress, an emerging focus in recent studies[40].

Frequency and duration of compound events. Having considered both daytime and nighttime heat stress thus far, the next component of the analysis focuses on changes in the frequency and duration of compound events, defined here as sequences of consecutive heat stress days and tropical nights.

To identify such events, we used the tropical night masks described above for the 1970s and the most recent decade (2015–2024). In parallel, we constructed daily masks for strong heat stress days, retaining only land grid cells where the daily maximum UTCI reached at least 32 °C. For each day, these two masks were combined to isolate grid cells experiencing both strong daytime heat stress and a tropical night within the same 24-h period.

For each decade (the 1970s and 2015–2024), and for each land grid cell, sequences of consecutive days meeting this compound event criterion were identified, and the duration (in days) of each sequence was recorded. Compound events were then aggregated into duration bins ranging from 1 day (that is, 1 day and 1 night) to up to a full year (271–365 days), yielding the total frequency of events of different durations across all days and all land grid cells within each continent, and for the globe as a whole. To account for hemispheric differences in seasonality, results for Africa were calculated separately for the northern and southern hemispheres. For each region and compound event duration bin, a multiplication factor was derived as the ratio of event counts in the most recent decade to those in the 1970s.

Population exposure to heat stress. To quantify changes in population exposure to heat stress over time, we combined ERA5-HEAT UTCI data with the 'Hybrid gridded demographic data for the world' dataset[18], again comparing the most recent decade (2015–2024) with the 1970s. As the population dataset is available in 5-year intervals, data from 1975 were used to represent the population in the 1970s, and data from 2020 to represent the most recent decade. The total population across all age bands was used. The total global population statistics are noted in Fig. 6 for 1975 and 2020, and agree well with other sources and datasets.

Population exposure was quantified through two complementary metrics. First, the total person-days of heat exposure were calculated for each grid cell by multiplying the decadal average annual number of heat stress days by the population in the corresponding grid cell, and summing globally. This was done for both the 1970s and the last 10 years (2015–2024), and for three heat stress thresholds; at least strong (≥32 °C), very strong (≥38 °C) and extreme (≥46 °C). The results for the most recent decade (2015–2024) are mapped in Extended Data Fig. 4.

Second, to assess the scale of exposure to sustained heat, we evaluated the number of people living in locations that exceeded a minimum number of heat stress days per year, in the 1970s compared with the last 10 years (2015–2024). For each threshold of ≥1, ≥10, ≥14, ≥30 and ≥90 days, a binary mask was applied to identify grid cells where the decadal average annual number of heat stress days exceeded the specified count of heat stress days, again for the same three heat stress thresholds. The exposed population was then computed by summing the population across those grid cells and normalizing by the total global population for the corresponding decade.

As part of this analysis, the increase in exposure to heat stress between the 1970s and the last 10 years (2015–2024) was decomposed into the increase caused by population growth (and redistribution) and the increase caused by changes in heat stress. This was done using counterfactual decomposition. First, the exposure in the 1970s was computed as outlined above, combining the population and heat stress days data for the 1970s. Second, a counterfactual scenario was computed, combining the population in 2020 with the heat stress days data for the 1970s, to assess the exposure if the climate had remained the same but population growth and redistribution had occurred as observed. Comparing these gives the increase in exposure due to population growth. Finally, the exposure in the last 10 years was computed, combining the population and heat stress days data for 2015–2024. Comparing this with the counterfactual scenario gives the increase in population exposed due to changes in heat stress.

Expressing exposure as a proportion of the total population at the time, rather than as an absolute number, reduces the influence of population growth over time, as absolute exposed population inevitably increases with global population growth; percentage exposure, by

contrast, reflects the share of the population experiencing hazardous heat and is therefore more indicative of climate-driven changes in heat stress exposure.

Several limitations should be acknowledged when interpreting the exposure estimates produced by this analysis. The method relies on gridded population snapshots taken at a single reference year for each decade, which cannot capture intradecadal demographic changes, such as migration or urbanization. The exposure metrics are also sensitive to the spatial and temporal resolution of the underlying datasets. Given ERA5-HEAT limitations in capturing extremes and microclimates such as urban heat islands[26], the exposure estimates are likely to be conservative. Historical population reconstructions, particularly in earlier decades, may depend on sparse or inconsistent census inputs, introducing additional uncertainty when comparing population exposure across decades. Finally, while expressing exposure as a percentage of the global population helps to separate population growth from climate-driven changes, it cannot completely disentangle the combined effects of spatial population redistribution and growth, and changing patterns of heat stress.

Reporting summary

Further information on research design is available in the Nature Portfolio Reporting Summary linked to this article.

Data availability

All datasets used in this study are freely and openly available. ERA5 reanalysis data can be downloaded from the Copernicus Climate Data Store (https://cds.climate.copernicus.eu). The ERA5 daily minimum 2-m air temperature data are available at https://cds.climate.copernicus.eu/datasets/derived-era5-single-levels-daily-statistics, and the ERA5-HEAT UTCI hourly data alongside postprocessed statistics such as daily/monthly/seasonal/annual maximum and minimum values and counts of heat/cold stress days are available at https://cds.climate.copernicus.eu/datasets/derived-utci-historical. These data can also be explored interactively using Thermal Trace (thermaltrace.climate.copernicus.eu). The 'Hybrid gridded demographic data for the world, 1950–2020'(ref. 18) dataset (0.25° resolution) is available via Zenodo at https://zenodo.org/records/6011021 (ref. 18).

Code availability

The Python and bash scripts (which make use of Climate Data Operators (CDO)) used in the data analysis are available from the corresponding author upon reasonable request.

References

37. Hersbach, H. et al. The ERA5 global reanalysis. *Q. J. R. Meteorol. Soc.* **146**, 1999–2049 (2020).
38. Soci, C. et al. The ERA5 global reanalysis from 1940 to 2022. *Q. J. R. Meteorol. Soc*. https://doi.org/10.1002/qj.4803 (2024).
39. Lopes, F. M., Dutra, E. & Boussetta, S. Evaluation of daily temperature extremes in the ECMWF operational weather forecasts and ERA5 reanalysis. *Atmosphere* **15**, 1 (2024).
40. Gong, P. et al. Action on hot nights: a scoping review of nighttime heat thresholds and their critical role in urban climate resilience. *Sustain. Cities Soc*. https://doi.org/10.1016/j.scs.2026.107303 (2026).

Author contributions

R.E. conceived and posed the research question, and all authors contributed to the study design. R.E. carried out the data analysis with support from J.N. A.L. and R.E. co-created the figures. All authors contributed to discussion and interpretation of the results. R.E. wrote the paper with input and review from all authors.

Funding

This research has been partially supported by the Copernicus Climate Change Service (C3S), which is implemented by ECMWF on behalf of the European Commission. C.D.N. acknowledges funding from Destination Earth, which is a European Union funded initiative and is implemented by ECMWF, ESA and EUMETSAT, and from the TRIGGER and ISMED-CLIM projects, which have received funding from the European Union under grant agreements 101057739 and 101156653, respectively.

Competing interests

The authors declare no competing interests.

Additional information

Extended data is available for this paper at https://doi.org/10.1038/s41558-026-02670-5.

Supplementary information The online version contains supplementary material available at https://doi.org/10.1038/s41558-026-02670-5.

Correspondence and requests for materials should be addressed to Rebecca Emerton.

Peer review information *Nature Climate Change* thanks Bogdan Antonescu, Dominic Royé and Warner van Kersen for their contribution to the peer review of this work. Peer reviewer reports are available.

https://doi.org/10.1038/s41558-026-02670-5

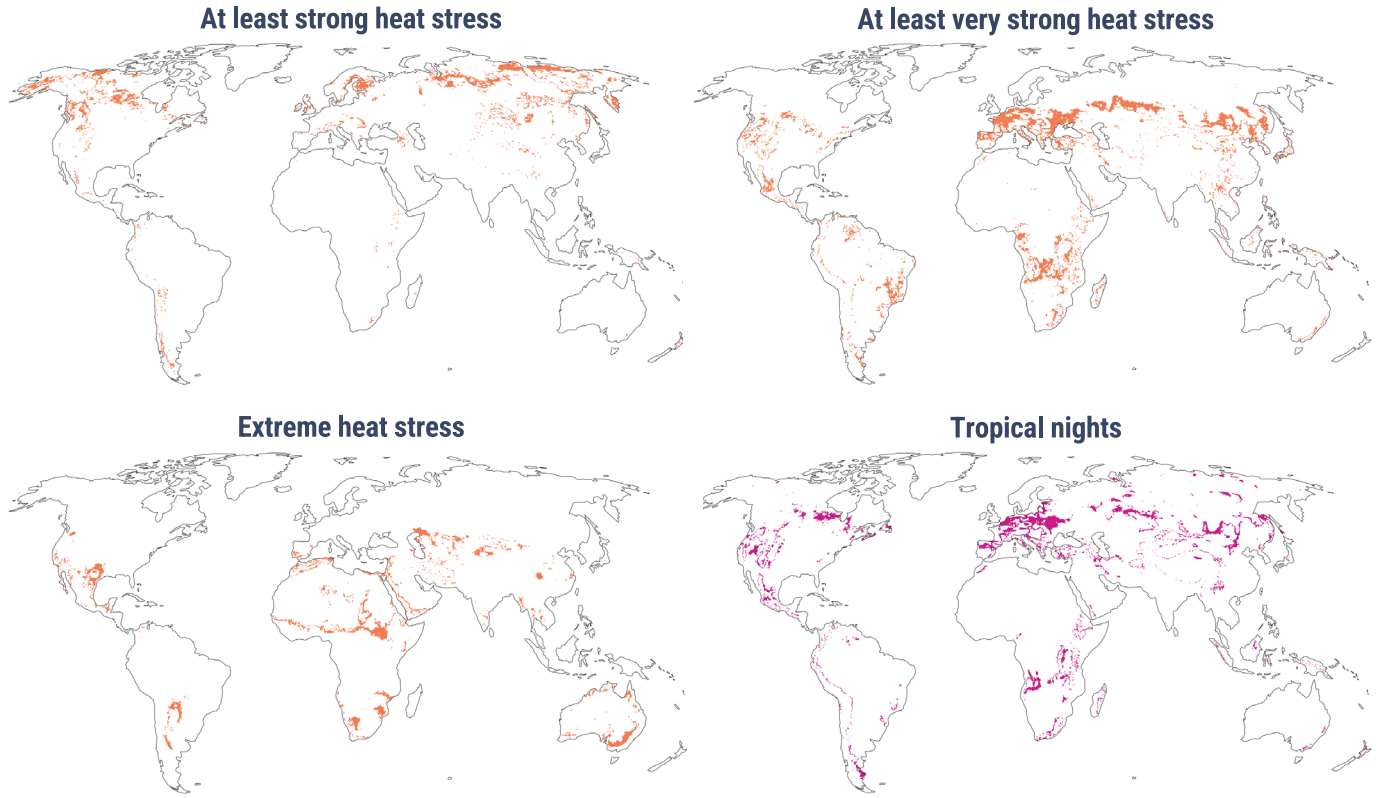

Extended Data Fig. 1 | The expanding footprint of heat stress. Coloured areas indicate locations that had an average of zero heat stress days or tropical nights in the 1970s, but that in the last ten years (2015–2024) recorded a non-zero average annual number of such days or nights. Results are shown for three categories of heat stress: at least strong (UTCI ≥ 32 °C), very strong (UTCI ≥ 38 °C) and extreme (UTCI ≥ 46 °C), and for tropical nights (minimum temperature ≥ 20 °C). Basemap data from Natural Earth (https://www.naturalearthdata.com).

https://doi.org/10.1038/s41558-026-02670-5

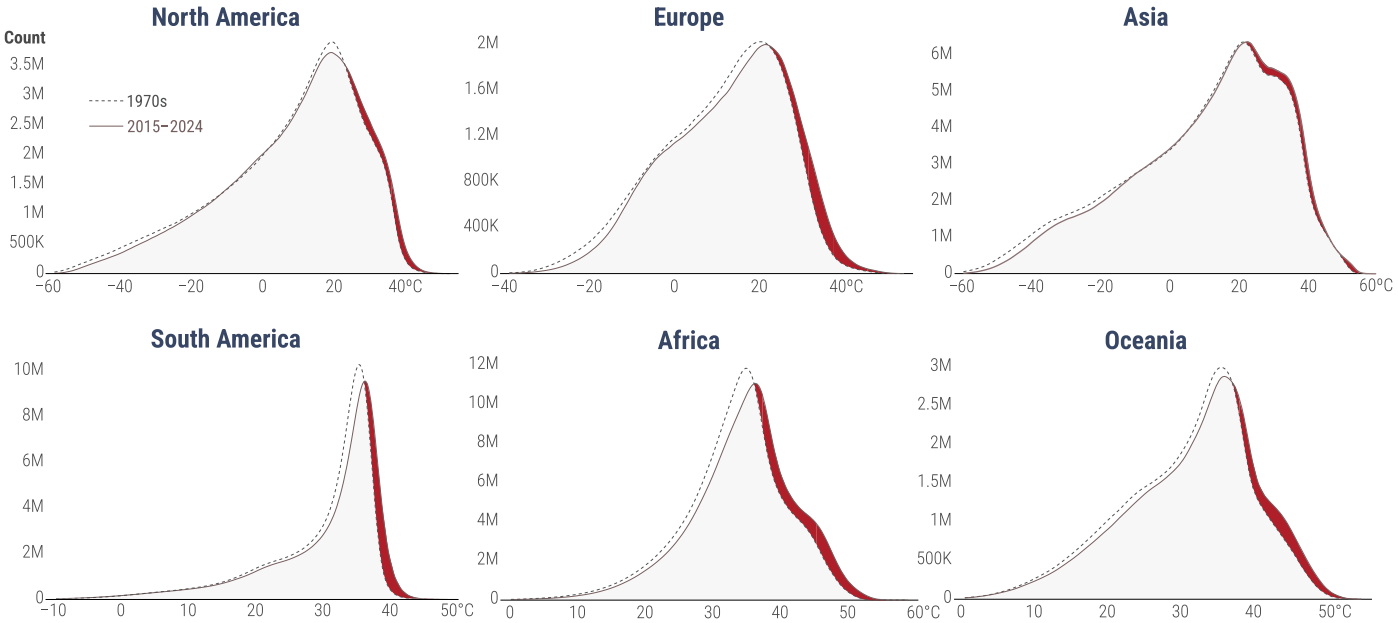

Extended Data Fig. 2 | Frequency distribution of feels-like temperatures (UTCI) for each continent in the 1970s and the last ten years (2015–2024). Frequency is defined as the total number of occurrences, calculated as the sum across all grid cells and days within two periods: the 1970s and the last ten years (2015–2024). The counts displayed are therefore shown in grid-cell-days. The red shaded areas highlight the shift of the distributions towards more extreme values.

https://doi.org/10.1038/s41558-026-02670-5

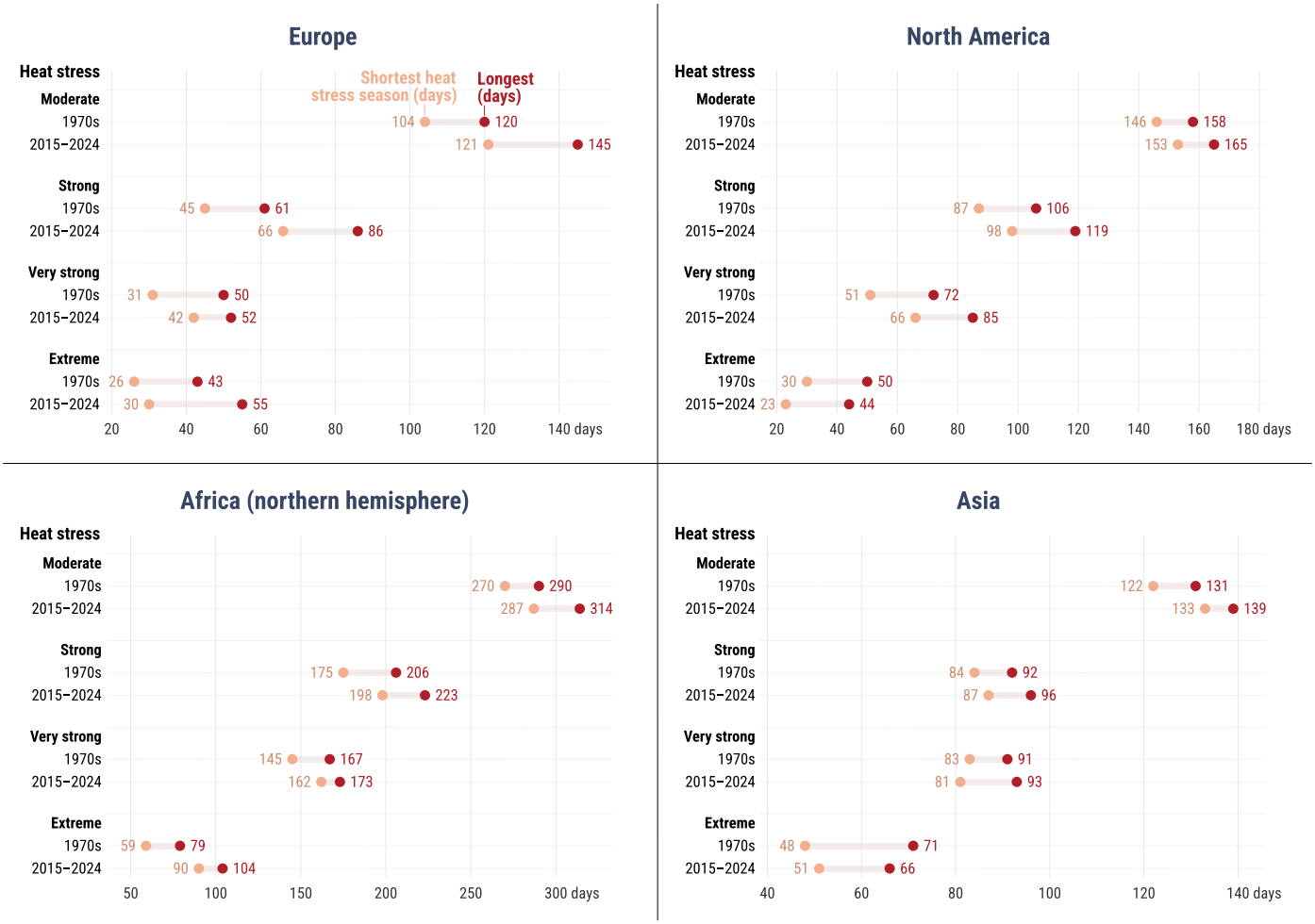

Extended Data Fig. 3 | Variability in the duration of the heat stress season. For each continent in the northern hemisphere, the duration in days of the shortest and longest heat stress season in the 1970s and in the last ten years (2015–2024), for four heat stress thresholds (moderate (≥ 26 °C UTCI), strong (≥ 32 °C UTCI), very strong (≥ 38 °C UTCI) and extreme (≥ 46 °C UTCI) heat stress). Due to the year-round presence of lower categories of heat stress in the tropics and less defined seasonality, the tropics are excluded from this analysis.

https://doi.org/10.1038/s41558-026-02670-5

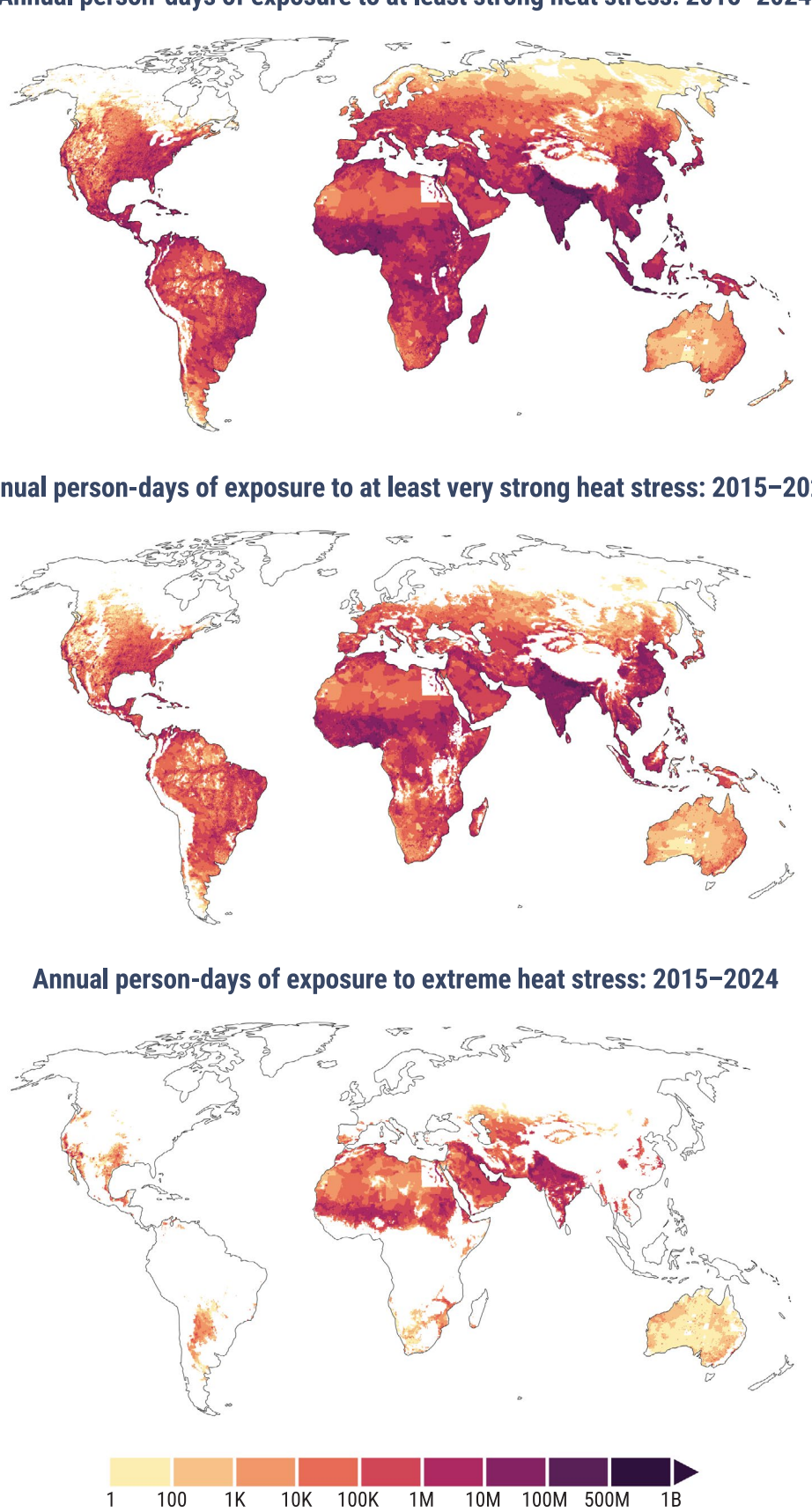

Extended Data Fig. 4 | Annual person-days of exposure to heat stress in the last ten years. Annual person-days (number of days x exposed population) of exposure to at least very strong (≥32 °C UTCI), very strong (≥38 °C UTCI) and extreme (≥46 °C UTCI) heat stress in the last ten years (2015–2024). Basemap data from Natural Earth (https://www.naturalearthdata.com).

https://doi.org/10.1038/s41558-026-02670-5

Extended Data Table 1 | Changes in the frequency of heat stress for the IPCC AR6 WGI reference regions

Change in frequency of strong, very strong and extreme heat stress from the 1970s to the last ten years (2015–2024)

For the IPCC AR6 WGI reference regions

Continent	Region	Region name	MF UTCI >32°C		MF UTCI >38°C		MF UTCI >46°C	
Europe								
	EEU	E.Europe	1.5	•••	2.5	•••	7.8	•
	NEU	N.Europe	2.1	•	71.7	•		
	WCE	Western&Central-Europe	2.8	•••	14.5	•		
	MED	Mediterranean	1.3	•••	1.6	•••	2.1	•••
Africa								
	CAF	Central-Africa	1.0	X	2.0	••	2.3	•
	ESAF	E.Southern-Africa	1.2	•••	1.8	•••	9.8	X
	NEAF	N.Eastern-Africa	1.1	X	1.5	•••	3.4	•
	SEAF	S.Eastern-Africa	1.2	•••	1.5	•••		
	WAF	Western-Africa	1.0	X	1.3	•••	2.2	•
	WSAF	W.Southern-Africa	1.2	•••	1.9	•••	6.1	X
	MDG	Madagascar	1.1	••	2.0	••		
	SAH	Sahara	1.1	X	1.1	••	1.8	•••
Asia								
	EAS	E.Asia	1.2	•••	1.6	•••	11.2	•
	ECA	E.C.Asia	1.2	•••	1.5	•••	3.0	•
	SAS	S.Asia	1.0	•••	1.1	••	0.9	•••
	WCA	W.C.Asia	1.1	•••	1.2	•••	1.5	•••
	ARP	Arabian-Peninsula	1.1	••	1.1	•••	1.5	•••
	TIB	Tibetan-Plateau	1.1	••	1.1	X	0.6	••
	RFE	Russian-Far-East	1.8	••	3.8	X		
	RAR	Russian-Arctic	1.9	•	0.2	X		
	ESB	E.Siberia	1.9	•••	4.0	•		
	WSB	W.Siberia	1.4	•••	1.7	•••	3.0	•
	SEA	S.E.Asia	1.0	X	1.5	••	5.1	X
Oceania								
	CAU	C.Australia	1.1	•••	1.2	•••	1.7	•••
	EAU	E.Australia	1.2	•••	1.6	•••	3.7	•
	NAU	N.Australia	1.1	•	1.2	•••	1.8	••
	SAU	S.Australia	1.1	•••	1.2	•••	1.8	•••
	NZ	New-Zealand	1.6	•	0.5	X		
C&S America								
	NCA	N.Central-America	1.2	•••	1.5	•••	1.7	••
	NES	N.E.South-America	1.1	X	2.2	••		
	NSA	N.South-America	1.0	X	2.7	•	40.0	X
	NWS	N.W.South-America	1.1	X	2.5	•	20.8	X
	SAM	South-American-Monsoon	1.0	X	2.2	••	87.4	X
	SCA	S.Central-America	1.1	•	1.9	••	4.8	•
	SES	S.E.South-America	1.2	•••	1.7	•••	2.4	••
	SSA	S.South-America	1.5	•••	2.0	••	1.6	X
	SWS	S.W.South-America	1.7	••	2.4	•	2.3	X
N America								
	CNA	C.North-America	1.2	•••	1.6	•••	48.5	X
	ENA	E.North-America	1.2	•••	1.6	••	0.4	X
	NEN	N.E.North-America	1.7	••	1.9	X		
	NWN	N.W.North-America	2.3	••	7.6	••		
	WNA	W.North-America	1.3	•••	1.7	•••	2.4	••
	CAR	Caribbean	1.1	•	2.4	••		

Multiplication factor (MF): how many times greater the frequency is in the last ten years, relative to the 1970s.
Dots indicate the statistical significance of the multiplication factors: $p < 0.001$ (•••), $p < 0.01$ (••), $p < 0.05$ (•), $p > 0.05$ (X)

Change in frequency of heat stress for each of the IPCC AR6 WGI reference regions, based on the daily maximum Universal Thermal Climate Index (UTCI) exceeding thresholds for strong (≥32°C), very strong (≥38°C), and extreme (≥46°C) heat stress. Change in frequency is indicated by the multiplication factor (MF), showing how much more often these thresholds were exceeded in 2015–2024 than in the 1970s. The statistical significance is indicated by the dots: $p < 0.001$ (•••), $p < 0.01$ (••), $p < 0.05$ (•). An X indicates $p > 0.05$. Statistical significance was assessed using a two-sided paired t-test comparing per-bin frequency counts above each threshold between the 1970s and the last ten years (paired across temperature bins). Multiplication factors are computed from the summed counts above each threshold. No adjustment for multiple comparisons was applied. Ocean regions, Antarctica and Greenland are not included.

https://doi.org/10.1038/s41558-026-02670-5

Extended Data Table 2 | Changes in the frequency of compound heat stress days and tropical nights

Compound event duration (days)	Global	Europe	Africa (northern hemisphere)	Africa (southern hemisphere)	North America	South America	Asia	Oceania
1	0.99 ± 0.001	1.73 ± 0.014	0.76 ± 0.002	1.19 ± 0.004	1.18 ± 0.004	0.91 ± 0.002	1.06 ± 0.003	1.08 ± 0.003
2	1.00 ± 0.002	1.81 ± 0.022	0.81 ± 0.003	1.21 ± 0.006	1.16 ± 0.007	0.95 ± 0.004	1.07 ± 0.004	1.06 ± 0.005
3	1.01 ± 0.002	1.84 ± 0.031	0.85 ± 0.003	1.21 ± 0.007	1.19 ± 0.009	0.94 ± 0.005	1.06 ± 0.005	1.05 ± 0.006
4-7	1.01 ± 0.002	2.15 ± 0.030	0.85 ± 0.003	1.24 ± 0.006	1.23 ± 0.007	0.93 ± 0.003	1.09 ± 0.004	0.99 ± 0.004
8-14	1.03 ± 0.002	2.59 ± 0.059	0.89 ± 0.004	1.27 ± 0.008	1.18 ± 0.010	0.94 ± 0.004	1.16 ± 0.006	1.03 ± 0.006
15-30	1.06 ± 0.003	3.37 ± 0.144	0.92 ± 0.005	1.41 ± 0.012	1.14 ± 0.013	1.00 ± 0.005	1.19 ± 0.007	1.02 ± 0.007
31-90	1.12 ± 0.004	2.35 ± 0.131	0.92 ± 0.006	1.57 ± 0.018	1.40 ± 0.020	1.10 ± 0.006	1.16 ± 0.009	1.17 ± 0.010
91-120	1.17 ± 0.008	1.79 ± 0.155	1.12 ± 0.012	1.65 ± 0.056	1.50 ± 0.055	1.06 ± 0.017	1.25 ± 0.021	1.11 ± 0.026
121-180	1.36 ± 0.009	-	1.39 ± 0.011	1.76 ± 0.072	1.74 ± 0.082	1.35 ± 0.020	1.04 ± 0.015	1.05 ± 0.028
181-270	1.64 ± 0.016	-	2.14 ± 0.031	1.85 ± 0.116	3.45 ± 0.399	1.05 ± 0.019	2.40 ± 0.062	1.53 ± 0.069
271-365	1.70 ± 0.038	-	2.82 ± 0.133	2.84 ± 0.499	-	1.50 ± 0.045	1.48 ± 0.168	1.13 ± 0.084

This table supports Fig. 5. Varying durations of compound heat stress days and tropical nights are indicated, together with multiplication factors showing how much more often these durations of compound events occurred in 2015–2024 than in the 1970s, for the globe and each continental region. Values>1 indicate an increased frequency in the last ten years compared to the 1970s, and values<1 indicate a decreased frequency. 95% confidence intervals are provided for each multiplication factor.

nature portfolio

Corresponding author(s): Rebecca Emerton

Last updated by author(s): May 12, 2026

Reporting Summary

Nature Portfolio wishes to improve the reproducibility of the work that we publish. This form provides structure for consistency and transparency in reporting. For further information on Nature Portfolio policies, see our Editorial Policies and the Editorial Policy Checklist.

Please do not complete any field with "not applicable" or n/a. Refer to the help text for what text to use if an item is not relevant to your study.
For final submission: please carefully check your responses for accuracy; you will not be able to make changes later.

Statistics

For all statistical analyses, confirm that the following items are present in the figure legend, table legend, main text, or Methods section.

n/a	Confirmed	
☐	☒	The exact sample size (*n*) for each experimental group/condition, given as a discrete number and unit of measurement
☒	☐	A statement on whether measurements were taken from distinct samples or whether the same sample was measured repeatedly
☐	☒	The statistical test(s) used AND whether they are one- or two-sided *Only common tests should be described solely by name; describe more complex techniques in the Methods section.*
☒	☐	A description of all covariates tested
☐	☒	A description of any assumptions or corrections, such as tests of normality and adjustment for multiple comparisons
☐	☒	A full description of the statistical parameters including central tendency (e.g. means) or other basic estimates (e.g. regression coefficient) AND variation (e.g. standard deviation) or associated estimates of uncertainty (e.g. confidence intervals)
☐	☒	For null hypothesis testing, the test statistic (e.g. *F*, *t*, *r*) with confidence intervals, effect sizes, degrees of freedom and *P* value noted *Give P values as exact values whenever suitable.*
☒	☐	For Bayesian analysis, information on the choice of priors and Markov chain Monte Carlo settings
☒	☐	For hierarchical and complex designs, identification of the appropriate level for tests and full reporting of outcomes
☒	☐	Estimates of effect sizes (e.g. Cohen's *d*, Pearson's *r*), indicating how they were calculated

Our web collection on statistics for biologists contains articles on many of the points above.

Software and code

Policy information about availability of computer code

Data collection	Python code was used to download data from the Copernicus Climate Data Store using the CDS API.
Data analysis	All data used in this study are open access and available to download freely online from e.g. the Copernicus Climate Data Store. To analyse the data, custom code was written using open software including Python (v 3.12.11), jupyter notebooks, and shell scripts to run analysis using cdo (climate data operators, v2.5.3)

For manuscripts utilizing custom algorithms or software that are central to the research but not yet described in published literature, software must be made available to editors and reviewers. We strongly encourage code deposition in a community repository (e.g. GitHub). See the Nature Portfolio guidelines for submitting code & software for further information.

Data

Policy information about availability of data

All manuscripts must include a data availability statement. This statement should provide the following information, where applicable:

- Accession codes, unique identifiers, or web links for publicly available datasets
- A description of any restrictions on data availability
- For clinical datasets or third party data, please ensure that the statement adheres to our policy

All datasets used in this study are freely and openly available. ERA5 reanalysis data can be downloaded from the Copernicus Climate Data Store (https://cds.climate.copernicus.eu). The ERA5 daily minimum 2m air temperature data are available at https://cds.climate.copernicus.eu/datasets/derived-era5-single-

levels-daily-statistics and the ERA5-HEAT UTCI hourly data alongside postprocessed statistics such as daily/monthly/seasonal/annual maximum and minimum values and counts of heat/cold stress days are available at https://cds.climate.copernicus.eu/datasets/derived-utci-historical. These data can also be explored interactively using Thermal Trace (thermaltrace.climate.copernicus.eu). The hybrid gridded demographic data for the world (18), 1950–2020 0.25° resolution dataset is available at https://zenodo.org/records/6011021.

Research involving human participants, their data, or biological material

Policy information about studies with human participants or human data. See also policy information about sex, gender (identity/presentation), and sexual orientation and race, ethnicity and racism.

Reporting on sex and gender	*Use the terms sex (biological attribute) and gender (shaped by social and cultural circumstances) carefully in order to avoid confusing both terms. Indicate if findings apply to only one sex or gender; describe whether sex and gender were considered in study design; whether sex and/or gender was determined based on self-reporting or assigned and methods used.* *Provide in the source data disaggregated sex and gender data, where this information has been collected, and if consent has been obtained for sharing of individual-level data; provide overall numbers in this Reporting Summary. Please state if this information has not been collected.* *Report sex- and gender-based analyses where performed, justify reasons for lack of sex- and gender-based analysis.*
Reporting on race, ethnicity, or other socially relevant groupings	*Please specify the socially constructed or socially relevant categorization variable(s) used in your manuscript and explain why they were used. Please note that such variables should not be used as proxies for other socially constructed/relevant variables (for example, race or ethnicity should not be used as a proxy for socioeconomic status).* *Provide clear definitions of the relevant terms used, how they were provided (by the participants/respondents, the researchers, or third parties), and the method(s) used to classify people into the different categories (e.g. self-report, census or administrative data, social media data, etc.)* *Please provide details about how you controlled for confounding variables in your analyses.*
Population characteristics	*Describe the covariate-relevant population characteristics of the human research participants (e.g. age, genotypic information, past and current diagnosis and treatment categories). If you filled out the behavioural & social sciences study design questions and have nothing to add here, write "See above."*
Recruitment	*Describe how participants were recruited. Outline any potential self-selection bias or other biases that may be present and how these are likely to impact results.*
Ethics oversight	*Identify the organization(s) that approved the study protocol.*

Note that full information on the approval of the study protocol must also be provided in the manuscript.

Field-specific reporting

Please select the one below that is the best fit for your research. If you are not sure, read the appropriate sections before making your selection.

☐ Life sciences ☐ Behavioural & social sciences ☒ Ecological, evolutionary & environmental sciences

Ecological, evolutionary & environmental sciences study design

All studies must disclose on these points even when the disclosure is negative.

Study description	This study uses global reanalysis datasets to assess changes in various aspects of heat stress across the globe, and uses a global gridded population dataset to additionally assess the global population exposure to different levels of heat stress for two decades, the 1970s and the most recent decade (2015-2024)
Research sample	The study uses reanalysis data at the global scale, and for all days and years from 1950 to 2024. For parts of the study, the 1970s and the most recent decade (2015-2024) are used to indicate the magnitude of change since the beginning of the increasing trend in heat stress (1970s) to now (the most recent decade). For some aspects of the study, the global dataset is split into different regions, such as the different continents, or IPCC regions, to ensure the best relevance to the particular aspect of the study.
Sampling strategy	Not really applicable - within the time periods of study and the regions identified, all data are used and samples are not decided based on sample size.
Data collection	Data was downloaded from the Climate Data Store or Zenodo. Extensive information on the creation of the reanlysis datasets is available in the literature, but this study was not involved in the creation of the datasets.
Timing and spatial scale	The study uses reanalyses data at the global scale, and for all days and years from 1950 to 2024. For parts of the study, the 1970s and the most recent decade (2015-2024) are used to indicate the magnitude of change since the beginning of the increasing trend in heat stress (1970s) to now (the most recent decade). For some aspects of the study, the global dataset is split into different regions, such as the different continents, or IPCC regions, to ensure the best relevance to the particular aspect of the study.
Data exclusions	Data were only excluded when they were beyond the boundaries of the relevant part of the study. For example, part of the study

Data exclusions	looks at changes in the length of the extreme heat season, but in the tropics there is no defined season, so the tropical are excluded from this part of the study. No data are permanently excluded from the whole study.
Reproducibility	All data used in this study is open source data and freely available for use. All methods are clearly included and fully extensive to ensure clarity of the methods and to ensure reproducibility. Some of the underlying data is available open acess in the new web application ' Thermal Trace', developed by C3S, which allows simple comparison of some aspects of the study and sense checking of the results as the heat stress data can be quickly and accessibly viewed and explored without even downloading data. The application does not provide interpretation of the data or combine the data and analyses in as much depth as the experiments and analysis in the paper, but provides completely open access to the underpinning datasets.
Randomization	Samples were not randomised. Samples were only selected for example to subset periods of time within the full dataset, such as taking all days within a certain decade, or to analyse data for certain regions of the globe.
Blinding	Given the nature of this study, blinding is not relevant to the analysis or the datasets involved.

Did the study involve field work? ☐ Yes ☒ No

Reporting for specific materials, systems and methods

We require information from authors about some types of materials, experimental systems and methods used in many studies. Here, indicate whether each material, system or method listed is relevant to your study. If you are not sure if a list item applies to your research, read the appropriate section before selecting a response.

Materials & experimental systems

n/a	Involved in the study
☒	☐ Antibodies
☒	☐ Eukaryotic cell lines
☒	☐ Palaeontology and archaeology
☒	☐ Animals and other organisms
☒	☐ Clinical data
☒	☐ Dual use research of concern
☒	☐ Plants

Methods

n/a	Involved in the study
☒	☐ ChIP-seq
☒	☐ Flow cytometry
☒	☐ MRI-based neuroimaging

Plants

Seed stocks	n/a - there may be an issue with the form, plants is ticked as n/a above as they are not involved in the study.
Novel plant genotypes	*Describe the methods by which all novel plant genotypes were produced. This includes those generated by transgenic approaches, gene editing, chemical/radiation-based mutagenesis and hybridization. For transgenic lines, describe the transformation method, the number of independent lines analyzed and the generation upon which experiments were performed. For gene-edited lines, describe the editor used, the endogenous sequence targeted for editing, the targeting guide RNA sequence (if applicable) and how the editor was applied.*
Authentication	*Describe any authentication procedures for each seed stock used or novel genotype generated. Describe any experiments used to assess the effect of a mutation and, where applicable, how potential secondary effects (e.g. second site T-DNA insertions, mosiacism, off-target gene editing) were examined.*